International Journal of Synergy in Engineering and Technology IJSET
Journal homepage: https://tatiuc.edu.my/ijset/index.php/ijset/ e-ISSN: 2735-0622

Study on Mechanical Properties of rHIPS/ABS/Saw Dust Using Box-Behnken Design with Maleic Anhydride Polypropylene

Adriana Muzale, Alias Mohd*, Zahari Deraman

Faculty of Engineering Technology, University College TATI, Jalan Panchor, Telok Kalong, 24000 Kemaman, MALAYSIA

*Corresponding author email: aliasmohd@uctati.edu.my

KEYWORDS

Composites
Mechanical Properties
Melt flow index test
Box-behnken design (BBD)
Maleic Anhydride Polypropylene (MAPP)

ABSTRACT

There is an increasing demand for sustainable materials due to the harm that plastic waste is causing to ecosystems and human health. An increasing market for high-tech material goods is driving materials research and development, particularly in the composite industry. The development of more environmentally friendly and economically viable materials is now possible due to recent increases in the study of the more effective commercial material sources available today. The purpose of this work is to determine the composition of rHIPS/ABS/sawdust composites and to examine their mechanical characteristics, notably impact and tensile strength. Standard test moulds ASTM D638 will be used to prepare the samples, and Box-Behnken Design (BBD) will be utilised for data analysis. The injection moulding machine has the following melting temperatures and cooling times: T1 is 200°C, T2 is 215°C, and T3 is 230°C (16–20 seconds). Three injection pressure levels will change during the moulding process: 100, 115, and 130 bar. The temperature of the mould will be maintained between 35°C and 40°C to control the cooling of the material that has been formed. According to the results, the maximum tensile strength is 102.6 MPa at 215°C melting temperature, 115 MPa pressure, and 18 seconds of cooling time. As for the data on tensile strength, the lowest result is 28.735 MPa at 230 °C for melting, 115 MPa for pressure, and 16 seconds for cooling. The maximum impact strength measured at 200 °C melting point, 130 MPa pressure, and 18 seconds of cooling time is 4.03 kJ/m^2. When the melting temperature is 200 °C, the pressure is 100 MPa, and the cooling time is 18 seconds, the lowest impact data is 2.76 kJ/m^2.

Received 21 February 2024; Revised 12 March 2024; Accepted 30 March 2024; Published 1 April 2024.

1.0 INTRODUCTION

The production of superior composites that meet specific requirements is challenging because of their intricate structures and short lifespans of two to three times. Although they can be recycled due to quality deterioration, waste polymer matrix composites are particularly challenging to recycle [1]. Important factors in the manufacture of composites include injection pressure, melting point, and cooling techniques. It is possible to produce composites with better mechanical and performance attributes by comprehending and optimizing these elements [2]. A range of natural fibers can be used in injection moulding to reinforce the composite [3].

Plastic injection moulded components are categorized using attribute quality metrics and variable (e.g., dimensions) [4]. Composites are particularly essential materials for a wide range of applications in several engineering domains because of their improved mechanical, physical, and machining properties. When compared to traditional materials, composite materials provide a number of benefits and superior properties that make them useful in a range of applications [5]. In order to create high-quality recycled plastics, recycling plastic wastes (PW) requires sorting waste according to certain physical characteristics, such as the types, colors, and forms of plastic [6][35]. Plastic pollution is a global issue that both developed and developing countries must address since it has a negative impact on ocean and landfill ecosystems [7]. HIPS is used in several industries, such as electrical instruments, automotive, and packaging [8].

Low-strength structural application material, high-impact polystyrene (HIPS; polybutadiene added to polystyrene during polymerization), is widely used for prototyping due to its accessibility, affordability, ease of manufacturing, machining, paint, and adhesive [10]. ABS is translucent, easily processed, and suitable for recycling and painting. It is widely used in many different applications, such as safety helmets, computer and information and communication technology (ICT) components, toys, electrical appliance housings, automobile body parts, wheel covers, instrument panels, and interiors, pipelines, and toys [9]. Global wastes from wood processing and exploitation operations are used to create sawdust materials. Significant attempts have been made over time to transform these materials into a carbon source that may be used to remediate wastewater [11]. In order to minimize environmental effects on ecosystems while maintaining technological and economic viability, the scientific and industrial communities have worked to produce ecological materials [12][31]. Additionally, it is mostly used as a heating material in homes or is abandoned to decompose [13]. One such biomass waste ash is sawdust, which has been studied by a number of researchers for usage as a stand-alone stabilizer, in combination with major binders like cement and lime, and for pozzolanic strength gain above primary binder stabilization alone [14][15].

To improve filler dispersion and remove moisture from matrices, a coupling agent is utilized. In addition to improving dimensional stability, a coupling agent can control the moisture content of the composites that are produced. To improve the connection of composite components, researchers and manufacturers frequently use commercially available silane compounds [16][17][18]. It has been researched to add coupling agents, like MAPP, to improve the interfacial adhesion between the constituents, which improves the mechanical properties and composite performance [19][20][34]. It is widely known that coupling agents, in particular, maleic anhydride-grafted polypropylene (MAPP), significantly improve the properties of manufactured panels and the bonding between wood fiber and polymer matrix. Nevertheless, the majority of these coupling agents are hazardous and costly [21][33][36]. Therefore, the current focus of research is on creating a high-quality coupling bio-agent for composites made of polymers and natural fibers.

In response surface methodology (RSM), the models are constructing depend on data in experimental design, describing the link among factors (independent parameters) and response (dependent parameters) [22]. These models (correlation) are utilized in evaluating the influence of factors, interactions on response and process optimization. In general, the results are described by 3D plot or by 2-D contour plot. The use of response surface methodology as optimization tool requires many stages which involve firstly factors chosen, method of experimentation, suitable model selection, checking of model adequacy, representation of model by graph and finally optimization to get optimum condition [23][24]. Box-Behnken design (BBD), a renowned approach under Response Surface Methodology (RSM), is chosen for process optimization due to its efficiency and adaptability [38][41]. BBD helps identify main components in a quadratic model, measure model goodness of fit, and boost experimental efficiency [25]. It reduces the number of experimental runs and provides insights into the response surface, aiding in finding optimal process conditions [26].

Tension testing is a material standard acceptance test that is often used to offer essential design information on the strength of materials. The ASTM D638 standard was used to perform tensile testing obtained by the injection moulding method [14][30]. Impact strength is a crucial metric in material science that defines a material's resistance to sudden, high-energy pressures [37]. Polymers, metals, and composite materials respond differently to fast loading due to differences in molecular organization, crystalline structure, and reinforcing chemicals [32]. Additionally, changes in processing processes, heat treatments, or alloying elements can significantly alter a material's ability to absorb and disperse energy upon impact [27]. The ASTM D256 and ISO 180 standards both recommend the Izod impact test over the Charpy test method [28]. The MFR test uses a closely defined extrusion plastometer to determine the rate of flow of molten polymer. Higher MFR dilutes the polymer, reducing processing temperature. The MFI is related to the viscosity of blend and is defined as the weight of the polymer extruded in 10 minutes through a specific capillary under specific temperature conditions [29].

2.0 EXPERIMENTAL PROCEDURE

2.1 Preparations of materials

The composite material was mostly composed of two kinds of polymers. First, there is Recycled High Impact Polystyrene (rHIPS), a thermoplastic material; second, there is Acrylonitrile-Butadiene-Styrene (ABS). The composite also included natural components in addition to the polymers. As seen in Figure 1, sawdust was utilised as a natural filler. Maleic anhydride polypropylene, or MAPP, was used as a coupling agent to improve the adhesion and bonding between the natural filler and the polymer matrix [39][40].

Recycled polystyrene is combined with different components to create Recycled High Impact Polystyrene (rHIPS), an eco-friendly composite material. As seen in Figure 1(b), the composite is crushed eight times during the manufacturing process to obtain a finer uniformity and optimise its qualities for a variety of applications. Meanwhile, composite materials with better properties are being made using sawdust, a byproduct of woodworking (Figure 1(c)). This economical and environmentally safe filler is utilised as reinforcement in many different industries, offering long-term solutions. To get the right consistency, mixing, sifting, and extrusion are used in the process.

(a)

(b)

(c)

(d)

Figure 1: Material used for the experiment, (a) ABS, (b) rHIPS, (c) Saw Dust, (d) MAPP

2.2 Parameters and levels for experimental works

The favourable technique for creating plastic components is injection moulding. Three crucial variables are regulated during the rHIPS/ABS/Saw Dust/MAPP composite injection moulding process: the melting temperature (200–230°C), the injection pressure (100–130 MPa), and the cooling duration (16–20 seconds) as shown in Table 1. The composite components' ability to combine is controlled by the melting temperature prior to injection, and the injection pressure ensures that the mould is fully filled without any errors. The cooling process aids in the moulded part's correct solidification and shape retention. For the production of superior composite materials with respectable mechanical properties that may be applied in numerous industries, it is essential to appropriately control these characteristics.

Table 1: Injection Moulding Parameters and levels

Parameter	Level
Melting Temperature (°C)	200-230
Injection Pressure (MPa)	100-130
Cooling Time (s)	16-20

3.0 RESULTS AND DISCUSSION

3.1 Formulation of Composite

Using twin-screw extrusion machines and the melt flow index (MFI) test, the study evaluated three formulations. Large blistering occurred during extrusion of the T3 formulation, leading to its exclusion from additional testing. But when the T1 and T2 formulations were evaluated using MFI, the T1 sample had encouraging qualities. This emphasizes how crucial the MFI test is for locating a viable formulation for more research or use. The composite result formulation is displayed in Table 2.

Table 2: Result of Formulation of Composite for rHIPS/ABS/Saw Dust/MAPP

Sample	**Composite**			**Coupling Agent**	**Range**
	rHIPS	ABS	Saw Dust	MAPP	
T1	20%	55%	20%	5%	Accepted
T2	30%	35%	30%	5%	Rejected
T3	40%	20%	35%	5%	Rejected

3.2 Melt Flow Index (MFI)

With an average Melt Flow Rate (MFR) of 7.08 (g/10 min) for all samples in Formula 1, there is little variation in the composite material. Table 3 demonstrates that Formula 1 has a more consistent MFI profile with minimal variance in MFR values across its samples, whereas Formula 2 exhibits a little bit more variability due to greater MFR values in samples 2 and 3. Nevertheless, Formula 2, as displayed in Table 4, yields MFI outcomes that are noticeably more varied, with individual samples displaying a greater range of MFR values. The MFR values of 8.4 for Samples 2 and 3 in Formula 2 are higher, indicating faster flow rates, possibly as a result of increased fluidity or ease of flow. All things considered while formulating the composites.

Table 3: Result MFI for Formula 1

Formula 1		
Composite	Weight (g)	MFR (g/10 min)
Sample 1	0.12	7.2
Sample 2	0.12	7.2
Sample 3	0.11	6.6
Sample 4	0.12	7.2
Sample 5	0.12	7.2
Average		7.08

Table 4: Result MFI for Formula 2

Formula 2		
Composite	Weight (g)	MFI (g/10 min)
Sample 1	0.13	7.8
Sample 2	0.14	8.4
Sample 3	0.14	8.4
Sample 4	0.12	7.2
Sample 5	0.11	6.6
Average		7.68

3.3 Mechanical Properties Analysis in RSM Box-Behnken Design (BBD)

Response Surface Methodology (RSM) data from a Box-Behnken design are shown in Table 5 to investigate the effects of melting temperature, pressure, and cooling duration on mechanical parameters, namely Tensile Strength and Impact Strength. The information is based on certain experimental runs in which various elements were adjusted in a methodical manner to see how they affected these properties. The measured attributes that correspond to each setting are displayed in the columns "Tensile Strength (MPa)" and "Impact Strength (kJ/m^2)", whereas the columns "Melting Temperature (°C)," "Pressure (MPa)," and "Cooling Time (s)" show the settings for these parameters in each run. The goal of the analysis is to pinpoint the crucial elements and the optimal amounts of each that have a substantial impact on the mechanical characteristics being studied.

The maximum tensile strength value recorded at a melting temperature of 215°C, pressure of 115 MPa, and cooling duration of 18 seconds is 102.6 MPa. Meanwhile, at 230 °C for melting, 115 MPa for pressure, and 16 seconds for cooling, the lowest value of the tensile strength data is 28.735 MPa. The maximum impact strength value reported for a melting temperature of 200 °C, pressure of 130 MPa, and cooling duration of 18 seconds is 4.03 kJ/m2. When the melting temperature is 200 °C, the pressure is 100 MPa, and the cooling time is 18 seconds, the lowest impact data is 2.76 kJ/m2.

Table 5: Experimental result for mechanical properties

Std	Run	Melting Temperature (°C)	Pressure (MPa)	Cooling time (s)	Tensile strength (MPa)	Impact strength (kJ/m2)
11	1	215	100	20	42.535	3.585
3	2	200	130	18	46.98	4.03
6	3	230	115	16	28.735	3.2
13	4	215	115	18	102.6	3.46
1	5	200	100	18	42.43	2.76
14	6	215	115	18	47.16	3.14
15	7	215	115	18	47.44	3.33
10	8	215	130	16	70.41	3.645
16	9	215	115	18	44.795	3.01
17	10	215	115	18	31.79	2.82
7	11	200	115	20	48.55	3.33
5	12	200	115	16	76.67	3.27
8	13	230	115	20	43.79	3.135
12	14	215	130	20	52.725	2.825
9	15	215	100	16	41.7	2.82
2	16	230	100	18	79.3	3.2
4	17	230	130	18	54.475	3.01

3.4 ANOVA for Tensile Strength Quadratic Model

The results of a Box-Behnken Design of Analysis are shown in Table 6. This analysis evaluated the impact of variables (C-Cooling Time, A-Melting Temperature and B-Injection Moulding Pressure) and their interactions (AB, AC, and BC) on a response variable, mostly mechanical properties. With an F-value of 0.1732 and a p-value of 0.9909, the "Model" row assesses the overall significance of the model and indicates that it is not statistically significant at a conventional significance level (such as 0.05). The significance of each component and how they relate to one another is thus established. To illustrate, the different factors and their interactions are represented that correspond to A, B, C, AB, AC, BC, A2, B2, and C2.

The F-values and corresponding p-values show how important each factor or interaction is in affecting the response variable. For example, a factor or interaction is considered significant if the p-value is less than a predetermined significance level, which is often 0.05. The "Lack of Fit" row evaluates how well the model matches the data. It is preferable to have a non-significant lack of fit (p-value > 0.05), which shows that the model accurately represents the data.

Table 6: Analysis of variance (ANOVA) for tensile strength

Source	Sum of Squares	df	Mean Square	F-value	p-value
Model	1034.19	9	114.91	0.1732	0.9909
A	8.67	1	8.67	0.0131	0.9122
B	43.36	1	43.36	0.0654	0.8056
C	111.86	1	111.86	0.1686	0.6936
AB	215.72	1	215.72	0.3252	0.5863
AC	466.02	1	466.02	0.7024	0.4297
BC	85.75	1	85.75	0.1292	0.7298
A^2	1.97	1	1.97	0.003	0.9581
B^2	12.5	1	12.5	0.0188	0.8947
C^2	90.54	1	90.54	0.1365	0.7227
Residual	4644.01	7	663.43		
Lack of Fit	1617.08	3	539.03	0.7123	0.5936
Pure Error	3026.93	4	756.73		
Cor Total	5678.2	16			

A-Melting Temperature; B-Injection Moulding Pressure; C-Cooling Time

3.5 Surface Plot for Tensile Strength Analysis

To display the trend of change in response within the specified range of input parameters as well as the impact of each parameter on the other parameters, 2-D and 3-D charts can be made for a variety of parameter combinations. The interaction between injection moulding pressure, tensile strength, and melting temperature is depicted in the graph in Figure 2. The predicted tensile strengths for different combinations of temperature and pressure are shown by the curved surface, with dots above or below the surface denoting discrepancies between actual measurements and predictions. The optimal conditions for maximal tensile strength are represented by the surface's peak, which is around 102.6 MPa.

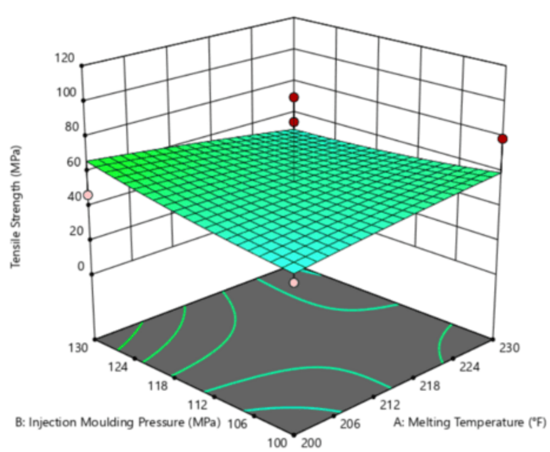

Figure 2: 3D Graph of Tensile Strength Analysis

Plotting the expected and measured values, the ideal line acts as a reference line. Each response's measured values are displayed, and the model's accuracy (fitness) is indicated by how close each value is to the ideal line. If every measured result is in line with or nearly so from the ideal line, the model generated for each answer is considered correct. The expected and experimental values are, for the most part, nearly the same, with very slight deviations. The optimal plot is located at Externally Studentized Residuals: 0.508 and Normal % Probability: 676.6, according to Figure 3 (a) Normal Residual Plot. In contrast, the optimal plot for 3 (b) Residual vs. Predicted is Externally Studentized Residuals: 0.51 and Predicted: 45.80.

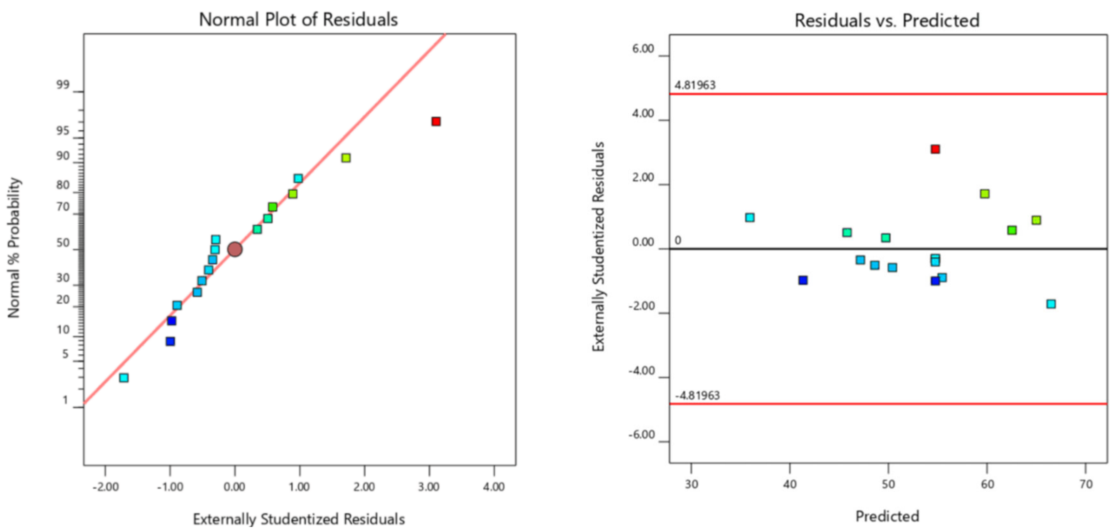

(a) (b)

Figure 3: The surface plot of ANOVA analysis (a) Normal Plot of Residual, (b) Residual vs Predicted

3.6 ANOVA for Impact Strength Quadratic Model

The impact strength study examines the effects of variables on a product's strength using a Box-Behnken design in response surface methodology (RSM) [34]. The correlations between parameters A (melting temperature), B (injection moulding pressure), and C (cooling time) and how they affect strength are shown in Table 7. Interestingly, the model, which consists of these elements and their combinations, is not significant ($p = 0.0929$), suggesting that these factors do not impact the overall degree of the effect.

While the remaining elements and their interactions are not significant, variables AB and BC alone ($p = 0.0183$ and $p = 0.0127$, respectively) show their combined influence on impact strength. Moreover, the model's lack of fit ($p = 0.5838$) highlights how well the model represents the observed data and demonstrates to its reliability. Further investigation into additional elements or interactions that can enhance this crucial attribute is required in light of the factors' potential limited influence on the product's impact strength within the examined ranges, as indicated by their lack of significance.

Table 7: Impact Strength Analysis (ANOVA)

Source	Sum of Squares	df	Mean Square	F-value	p-value
Model	1.44	9	0.1605	2.82	0.0929
A	0.0893	1	0.0893	1.57	0.2508
B	0.1639	1	0.1639	2.88	0.1336
C	0.0004	1	0.0004	0.0079	0.9317
AB	0.5329	1	0.5329	9.36	0.0183
AC	0.0039	1	0.0039	0.0686	0.8009
BC	0.6281	1	0.6281	11.03	0.0127
A^2	0.0134	1	0.0134	0.2361	0.6419
B^2	0.0073	1	0.0073	0.1274	0.7317
C^2	0.0027	1	0.0027	0.0471	0.8343
Residual	0.3986	7	0.0569		
Lack of Fit	0.1415	3	0.0472	0.7339	0.5838
Pure Error	0.2571	4	0.0643		
Cor Total	1.84	16			

A-Melting Temperature; B-Injection Moulding Pressure; C-Cooling Time

3.7 Surface Plot for Impact Strength Analysis

The graph in Figure 4 illustrates how strength is affected by injection moulding pressure and melting temperature when cooling time remains constant. The predicted impact strength for a range of melting temperatures and injection pressures is represented by the curved surface. Greater impact strength is implied by higher positions on the surface. Design points below the surface reveal lower-than-expected values, while those above the surface show that observed impact strengths were more than projected. The predicted impact strength for a range of melting temperatures and injection pressures is represented by the curved surface. Real impact strength readings are represented by the dots above and below the surface. Measurements that were higher than expected are indicated by red dots above the surface and lower than expected readings are indicated by blue dots below it. The predicted impact strength at the optimal melting temperature and injection pressure is represented by the highest point on the surface, which is approximately 4.03 kJ/m^2.

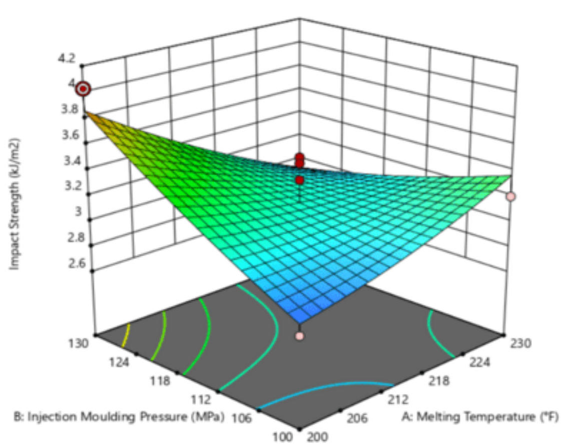

Figure 4: 3D Graph of Impact Strength Analysis

The ideal line serves as a reference line and depicts the measured and expected values. Each response's measured values are shown, and the model's accuracy (fit) is indicated by how close each value is to the ideal line. If all of the measured values are in line with or near the ideal line, the model created for each answer is deemed valid. The expected and experimental values are, for the most part, nearly the same, with just small variations. The optimal plot is Externally Studentized Residuals: -0.052 and Normal% Probability: 50.0, as shown in Figure 5 for (a)Normal Residual Plot. The optimal plot in (b) Residual vs. Predicted is Externally Studentized Residuals: 0.258 and Predicted: 3.167.

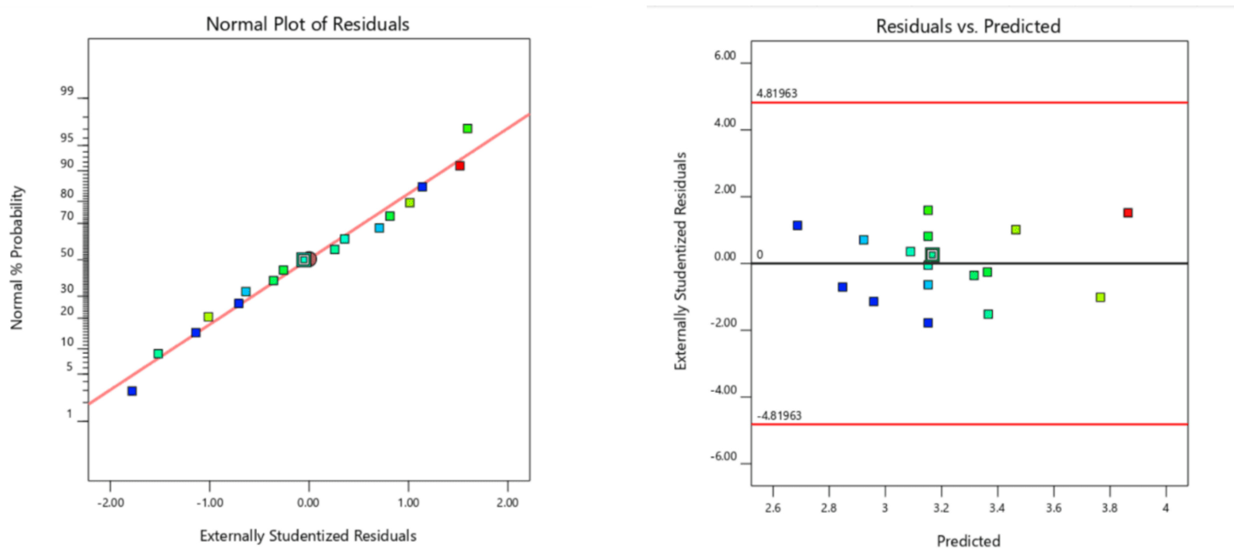

(a) (b)

Figure 5: The surface plot of ANOVA analysis (a) Normal Plot of Residual, (b) Residual vs Predicted.

4.0 CONCLUSIONS

The response surface method (RSM) was used in the study to assess mechanical parameters, which emphasizes the critical roles that variables like melting temperature, injection moulding pressure, and cooling time have in determining the mechanical properties of those composites. This highlights the importance of careful formulation evaluation and ongoing research efforts to advance sustainable composite materials, particularly in the fight against environmental issues related to plastic waste. Ultimately, the ANOVA results highlight the complexity and significance of further research in this area by providing unique insights into the subtle effects of individual components and their interactions on tensile strength and Impact strength within the rHIPS/ABS/sawdust composite framework. The experimental study that was presented demonstrated how well the injection moulding method that forms these composites with wood dust is suited for it. The current study set out to assess the mechanical characteristics of ABS and wood sawdust-reinforced rHIPS in order to create a composite. The investigations mentioned above lead to the following conclusions:

(i) The maximum tensile strength value recorded was 102.6 MPa, with the melting temperature being 215°C, the pressure being 115 MPa, and the cooling duration being 18 seconds. The data for the lowest value of tensile strength is 28.735 MPa, which is obtained at 230 °C for melting, 115 MPa for pressure, and 16 seconds for cooling.

(ii) The maximum impact strength data, at 200 °C for melting, 130 MPa for pressure, and 18 seconds for cooling, is 4.03 kJ/m2. When the melting temperature is 200 °C, the pressure is 100 MPa, and the cooling time is 18 seconds, the lowest impact data is 2.76 kJ/m2.

(iii) The current study's findings indicate that, with the right wood sawdust composition, it is possible to create wood sawdust composites with good mechanical qualities. Wood sawdust can be utilized in the rHIPS and ABS matrix as reinforcement and filler, which will lower costs and improve the environment.

(iv) Future studies on moisture absorption in composite materials should examine how moisture interacts with them over time and how this affects performance, durability, and structural integrity. This might shed light on the behavior of materials, real-world uses, and the creation of more durable materials. The optimized composite will be subjected to mechanical characterization and SEM examination.

Author Contribution

Adriana Muzale: Conceptualization, methodology, visualisation, writing and testing. Alias Mohd: Conceptualization, methodology, investigation, visualisation, writing, supervision and editing. Zahari Deraman: Sampling, supervision and testing.

Conflict of Interest

The authors declare that they have no known competing financial interests or personal relationships that could have appeared to influence the work reported in this paper.

Acknowledgements

The authors gratefully acknowledge the University College TATI (UC TATI) and everyone involved which made this work possible.

5.0 REFERENCES

[1] Fadare Olugbenga Babatunde, Adewuyi Benjamin Omotayo, Oladele Isiaka Oluwole, Kingsley Ukoba. A Review on Waste-wood Reinforced Polymer Matrix Composites for Sustainable Development, IOP Conf. Series: Materials Science and Engineering. 2021; 1107 (2021) 012057.

[2] Ferreira, E. da, Luna, C. B., Araújo, E. M., Siqueira, D. D., Wellen, R. M. Polypropylene/wood powder composites: Evaluation of PP viscosity in thermal, mechanical, thermomechanical, and morphological characters. Journal of Thermoplastic Composite Materials. 2019; 35(1), 71–92.

[3] M. S. Rabbi; Tansirul Islam; G. M. Sadiqul Islam. Injection-molded natural fiber-reinforced polymer composites–a review. 2021; https://doi.org/10.1186/s40712-021-00139-1

[4] Czepiel M, Bańkosz M, Sobczak-Kupiec A. Advanced Injection Molding Methods: Review. Materials (Basel). 2023 Aug 24;16(17): 5802.

[5] Sharma, A. K., Bhandari, R., Aherwar, A., & Rimašauskienė, R. Matrix materials used in Composites: A comprehensive study. Materials Today: Proceedings. 2020; 21, 1559–1562.

[6] P.G.C. Nayanathara Thathsarani Pilapitiya , Amila Sandaruwan Ratnayake. The world of plastic waste: A review. The world of plastic waste: A review. 2024.

[7] Kumar, S., Vedrtnam, A., & Pawar, S. J. Correction to: Effect of wood dust type on mechanical properties, wear behavior, biodegradability, and resistance to natural weathering of wood-plastic composites. Frontiers of Structural and Civil Engineering. 2021;15(4), 1071–1071.

[8] Wang, Feng; Chang, Li; Hu, Yanming; Wu, Guangfeng; Liu, Heng. Synthesis and Properties of In-Situ Bulk High Impact Polystyrene Toughened by High cis-1,4 Polybutadiene. Polymers. 2019; 11(5), 791.

[9] Chauhan, Vardaan; Kärki, Timo; Varis, Juha (). Review of natural fiber-reinforced engineering plastic composites, their applications in the transportation sector and processing techniques. Journal of Thermoplastic Composite Materials. 2019; 089270571988909.

[10] Sieradzka M, Fabia J, Biniaś D, Graczyk T, Fryczkowski R. High-Impact Polystyrene Reinforced with Reduced Graphene Oxide as a Filament for Fused Filament Fabrication 3D Printing. Materials (Basel). 2021 Nov 19;14(22):7008.

[11] Kayode Adesina Adegoke, Oreoluwa Ololade Adesina, Omolabake Abiodun Okon-Akan, Oyeladun Rhoda Adegoke, Abdullahi Biodun Olabintan, Oluwaseyi Aderemi Ajala, Halimat Olagoke, Nobanathi Wendy Maxakato, Olugbenga Solomon Bello. Sawdust-biomass based materials for sequestration of organic and inorganic pollutants and potential for engineering applications, Current Research in Green and Sustainable Chemistry. 2022; Volume 5,2022,100274.

[12] Wallisson Alves da Silva;Carlos Bruno Barreto Luna;João Baptista da Costa Agra de Melo;Edcleide Maria Araújo;Edson Antônio dos Santos Filho;Raimundo Nonato Calazans Duarte. Feasibility of Manufacturing Disposable Cups using PLA/PCL Composites Reinforced with Wood Powder. Journal of Polymers and the Environment. 2021.

[13] Kartal, İ. Effect of hornbeam sawdust size on the mechanical properties of Polyethylene Composites. Emerging Materials Research. 2020; 9(3), 979–984.

[14] M. Z. Umor , A. Mohd, M. Azwandy, Mechanical properties of wood dust and recycled polymers blends composition in injection moulding, RETREAT 2020 Journal of Physics: Conference Series 1874. 2021; 012066.

[15] James, J. Strength benefit of Sawdust/Wood Ash Amendment in cement stabilization of an expansive soil. Revista Facultad de Ingeniería. 2019; 28(50), 44–61.

[16] Azman Mohammad Taib, M. N., & Julkapli, N. M. Dimensional stability of natural fiber-based and hybrid composites. Mechanical and Physical Testing of Biocomposites, Fibre-Reinforced Composites and Hybrid Composites. 2019; 61–79.

[17] Kajaks, J., Kalnins, K., & Matvejs, J. Adhesion investigations of systems based on birch plywood and Wood Plastic Composites. Key Engineering Materials. 2020; 850, 76–80.

[18] Madhavi, S., Raju, N.V. & Johns, J. Characterization of Bamboo - Polypropylene Composites: Effect of Coupling Agent. Fibers Polym 22. 2021; 3183–3191.

[19] Foti, D., E. Voulgaridou, E., Karastergiou, S., R. Taghiyari, H., & N. Papadopoulos, A. Physical and mechanical properties of eco-friendly composites made from wood dust and recycled polystyrene. Journal of Renewable Materials. 2022; 10(1), 75–88.

[20] Ali, F. A., Hamzah, K., Khashi'ie, N. S., Waini, I., Mustafa, N., & Long, N. M. Mechanical and physical properties of sawdust-reinforced epoxy resin composites. Journal of Southwest Jiaotong University. 2022; 57(3), 292–299.

[21] Younesi-Kordkheili, H., & Pizzi, A. Nanolignin, a coupling bio-agent for wood-plastic composites. Journal of Renewable Materials. 2023; 11(5), 2075–2083.

[22] Nassiri Mahallati, M. Advances in modeling saffron growth and development at different scales. Saffron. 2020; 139–167.

[23] Breig, S. J., & Luti, K. J. Response surface methodology: A review on its applications and challenges in Microbial Cultures. Materials Today: Proceedings. 2021; 42, 2277–2284.

[24] Chen, B., Wang, X., Li, P., Feng, X., Mao, Z., Wei, J., Lin, X., Li, X., & Wang, L. Exploring the protective effects of freeze-dried lactobacillus rhamnosus under optimized cryoprotectants formulation. LWT. 2023; 173, 114295.

[25] Goren, A. Y., Recepoğlu, Y. K., & Khataee, A. Language of response surface methodology as an experimental strategy for electrochemical wastewater treatment process optimization. Artificial Intelligence and Data Science in Environmental Sensing. 2022; 57–92.

[26] Polat, S., & Sayan, P. Application of response surface methodology with a box–Behnken design for struvite precipitation. Advanced Powder Technology. 2019; 30(10), 2396–2407.

[27] Daskiran, E. G., Daskiran, M. M., & Gencoglu, M. Experimental investigation on impact strength of ar glass, basalt and PVA textile reinforced cementitious composites. European Journal of Environmental and Civil Engineering, 26(6). 2020; 2037–2056.

[28] Raj, S. S., Michailovich, K. A., Subramanian, K., Sathiamoorthyi, S., & Kandasamy, K. T. Philosophy of selecting ASTM standards for mechanical characterization of polymers and Polymer Composites. Materiale Plastice, 58(3)/ 2021; 247–256.

[29] Dewi, R., Sylvia, N., Zulnazri, & Riza, M. Melt flow index (MFI) analysis of sago based thermoplastic starch blend with polypropylene and polyethylene. Materials Today: Proceedings. 2023; 87, 396–400.
[30] Ad, M. A., Rochardjo, H. S., & Cahyo, B. (2019). Effects of processing parameters on the tensile strength of injection molding unidirectional glass fiber reinforced polypropylene composite. AIP Conference Proceedings.
[31] Kumar, R.; Verma, A.; Shome, A.; Sinha, R.; Sinha, S.; Jha, P.K.; Kumar, R.; Kumar, P.; Shubham; Das, S. (2021). Impacts of Plastic Pollution on Ecosystem Services, Sustainable Development Goals, and Need to Focus on Circular Economy and Policy Interventions. Sustainability 2021, 13, 9963.
[32] Abbas, E. N., Al-Waily, M., Hammza, T. M., & Jweeg, M. J. An investigation to the effects of impact strength on laminated notched composites used in prosthetic sockets manufacturing. IOP Conference Series: Materials Science and Engineering. 2020; 928(2).
[33] Ferede, E. Evaluation of mechanical and water absorption properties of alkaline-treated sawdust-reinforced polypropylene composite. Journal of Engineering. 2020; 1–8.
[34] Foppiano, M., Saluja, A., & Fayazbakhsh, K. The effect of variable nozzle temperature and cross-sectional pattern on interlayer tensile strength of 3D printed ABS specimens. Experimental Mechanics. 2021; 61(9), 1473–1487.
[35] Kosior, E., & Crescenzi, I. Solutions to the plastic waste problem on land and in the oceans. Plastic Waste and Recycling. 2020; 415–446.
[36] Madhavi, S., Raju, N. V., & Johns, J. Characterization of bamboo - polypropylene composites: Effect of coupling agent. Fibers and Polymers. 2021; 22(11), 3183–3191.
[37] Monti, M., Scrivani, M., Kociolek, I., Larsen, Å., Olafsen, K., & Lambertini, V. Enhanced impact strength of recycled PET/glass fiber composites. Polymers. 2021; 13(9), 1471.
[38] Nor, A. F., Hassan, M. Z., Rasid, Z. A., Aziz, S. A., Sarip, S., & Md Daud, M. Y. Optimization on tensile properties of kenaf/multi-walled CNT hybrid composites with box-behnken design. Applied Composite Materials. 2021; 28(3), 607–632.
[39] Ravikiran, B., Pradhan, D. K., Jeet, S., Bagal, D. K., Barua, A., & Nayak, S. Parametric optimization of plastic injection moulding for FMCG polymer moulding (PMMA) using hybrid Taguchi-WASPAS-Ant Lion Optimization algorithm. Materials Today: Proceedings. 2022; 56, 2411–2420.
[40] Teixeira, F. da, Peres, A. C., & Pacheco, E. B. Mechanical recycling of acrylonitrile-butadiene-styrene copolymer and high impact polystyrene from waste electrical and electronic equipment to comply with the circular economy. Frontiers in Sustainability. 2023; 4.
[41] Yiga, V. A., Lubwama, M., Pagel, S., Olupot, P. W., Benz, J., & Bonten, C. Optimization of tensile strength of PLA/clay/rice husk composites using box-behnken design. Biomass Conversion and Biorefinery. 2021; 13(13), 11727–11753.

